

Role of process parameters on bondability and pad damage indicators in copper ball bonding

I. Qin^a, A. Shah^{b,*}, C. Huynh^a, M. Meyer^a, M. Mayer^b, Y. Zhou^b

^a Kulicke and Soffa Industries Inc., Fort Washington, PA, USA

^b Microjoining Laboratory, University of Waterloo, Waterloo, ON, Canada

ARTICLE INFO

Article history:

Received 17 February 2010

Received in revised form 6 April 2010

Accepted 7 April 2010

Available online 6 May 2010

ABSTRACT

Cu wire bonding is one of the hottest trends in electronic packaging due to the cost and performance advantages of Cu wire over Au wire. However, there are many challenges to Cu wire bonding, one of which is the increased stress transmitted to the bond pad during bonding. This high stress is not desirable as it leads to pad damage or cratering in the Si under the pad. Another issue is pad splash in which the pad material is squeezed outside the bonded area, which in severe cases can cause Al pad thinning and depletion. To study the root cause of the increased stress, ball bonding is performed with Au and Cu wires using the same levels of ultrasound (USG), bonding force (BF), and impact force (IF). The bonding is performed on a bonding test pad with integrated piezoresistive microsensors and the in situ pad stress is measured in real time. The ultrasonic pad stress did not show any significant difference between the Au and the Cu ball bonding processes. This indicates that the cause of increased stress cannot be attributed to material properties such as hardness alone, and that the differences in bondability and bonding parameters required for the Cu process might be more influential. To achieve optimal bonding results in terms of shear force per unit area, the Cu process requires higher BF and USG settings, which are the main causes of pad damage. To understand the effect of bonding parameters IF, BF, and USG on pad stress, a detailed DOE is conducted with Cu wire. In addition to conventional bonding parameters, the effect of a non-zero USG level applied during the impact portion of the bonding (pre-bleed USG) is investigated. One of the findings is the reduction of pad damage when higher pre-bleed USG levels are used.

© 2010 Elsevier Ltd. All rights reserved.

1. Introduction

Thermosonic Au ball bonding has been the most preferred method for electrical connections to integrated circuits (ICs) [1–3]. In this process, a thin wire is welded to a metallization pad of an IC and to a substrate terminal, thereby interconnecting the IC with a larger scale substrate circuit. However, with the skyrocketing price of Au, the industry is continuously looking for a cheaper alternative to Au wire. Among the alternatives being developed, Cu wire is being increasingly used in the industry [4], followed by Pd coated Cu wire [5]. Other wire materials, in particular Au–Ag wire [6] have also been developed, however, it has not been widely adopted in production. The main reason for using Cu wire instead of Au is the cost saving: at the current reference Au price of \$1100–\$1200 per ounce, a 500 m spool of 20 μm Au wire costs \$200, which is about 10 times the cost of a comparable Cu wire. Moreover, Cu has superior electrical and thermal conductivities as well as higher mechanical strength [7–10]. The higher strength of Cu al-

lows for longer distances between the ball and the crescent bonds because the wire loop is more resistant to deformation.

However, there are a set of challenges that need to be solved before a robust Cu wire bonding process can be implemented in the industry. The first challenge is that Cu readily forms an oxide layer on its surface, which reduces its bondability. In order to limit the oxidation of Cu, the bonder must be retrofitted with a Cu kit that consists of a means of supplying a shielding gas during free air ball (FAB) formation process. The most common type of shielding gas used in Cu ball bonding is a homogeneous mixture of 95% N₂ and 5% H₂ [11]. The second challenge faced by Cu wire bonding is the narrow crescent bond process window. In particular, the short tail problems in Cu ball bonding caused by a weak tail bond [11] cause frequent production stops, lowering the mean-time between assists (MTBA). The third challenge is the increased risk of damage to the semiconductor chip due to the high hardness of Cu. Due to its higher hardness compared to Au wire, higher normal and ultrasonic forces are often used in Cu ball bonding, resulting in ≈30% higher bonding stress [12] acting at the bond pad. The higher pad stress increases the likelihood of chip damage such as pad cracking [13,14], pad splash [15–17], silicon cratering [18–20].

* Corresponding author. Tel.: +1 5198884567x33326.

E-mail address: ashah011@engmail.uwaterloo.ca (A. Shah).

This paper focuses on hardness related issues in Cu ball bonding to Al bond pad (Cu–Al process). It investigates the root causes of increased pad stress usually observed in Cu ball bonding. The designed experiments method is used to study the synergistic effect of various bonding parameters on bonding quality and pad splash. The goal is to identify the most influential parameters affecting the bonding quality and pad splash. Parts of this work have been presented in [21]. This work adds more information and discusses the results in greater detail.

2. Experimental setup

Thermosonic ball bonding is performed on Kulicke and Soffa (K&S) IConn automatic ball bonder using Au and Cu wires (W.C. Heraeus GmbH, Hanau, Germany), both 25.4 μm in diameter. The bonding is performed at a nominal heater plate temperature of 160 °C, resulting in actual bonding temperature of ≈138 °C measured at the pad surface. A standard ceramics bottleneck capillary (K&S part number 414FE-2063-R35) is used for bonding. A copper kit with forming gas is used to prevent oxidation of copper during free air ball (FAB) formation. The forming gas used is a homogeneous mixture of 95% Nitrogen and 5% Hydrogen. The flow rate of the forming gas is set to 0.62 l/min.

Two types of test chips are used for bonding: a K&S test chip and a microsensor test chip [12,22,23]. The K&S test device has Al metalized bond pads, about 0.8–1 μm thick, and without any passivation layer. This test device has known issues with adhesion of the Al pad to the oxide layer and is sensitive to pad lift after pull test. Thus, it is a good test vehicle to compare different wire bonding processes for pad lift and pad damage. However, some of results from the test device such as the number of pad lifts during pull test are not typical, and it is very likely to be worse than that observed in typical production devices.

2.1. Microsensor test chip

The test chip has integrated piezoresistive microsensors that are used to measure in situ ultrasonic and normal forces acting at the pad during the bonding process. The design and operation details of the microsensors and various electrical components integrated in the test chip are explained in detail in [24]. The microsensors were calibrated to measure the in situ ultrasonic [12] and normal forces [22] acting at the bond pad during the bonding. The microsensor is mounted to the die pad of a 16-pin ceramic small-outline integrated circuit (SOIC) package using a standard silver filled epoxy and cured in an oven at 150 °C for 60 min. The connection pads on the test chip are connected by Au ball bonds

to the package terminals, which are soldered to a printed circuit board (PCB) as shown in Fig. 1.

3. Bonding with same parameters

Ball bonding is performed with Au and Cu wires using same set of bonding parameters as shown in Table 1. The electronic flame off (EFO) firing time is adjusted for both Au and Cu wires so as to obtain FAB with similar diameters. Although these parameters are not optimal for either Au or Cu, it offers insights into the material impact on pad stresses. While these parameters result in an over-bonded (squashed) ball for the Au process, it results in an under-bonded ball for the Cu process. The results of bonding process with Au and Cu wires using same bonding parameters are given Table 2. As expected, the Cu ball bond shows lower shear strength compared to the Au ball bond. The average pull test value is higher for Cu ball bonding than for Au. This is due to the higher tensile strength of Cu compared to Au. However, the standard deviation is also high due to low pull strength measured when the pad lift occurs. While all the Au ball bonds failed at the neck during pull tests, 33.3% pad lifts are observed during the Cu bond pull tests. Thus, even with low bonding parameters, pad damage and pad material depletion (a result of pad splash) are issues during Cu wire bonding.

To study the material impact on the pad stresses, Au and Cu ball bonds are made with same parameters (Table 1) on the test pad with integrated microsensors as shown by example micrographs in Fig. 2a and b, respectively. Typical microsensor signals of ultrasonic and normal forces measured for the Au and Cu ball bonds made with same set of parameters are shown in Fig. 3a and b,

Table 1
Ball bonding parameters for same parameter test.

Parameter	Value
Contact threshold [machine unit]	10
Bond force [g]	14
Ultrasonic current [mA]	84
Time [ms]	10

Table 2
Process responses for same parameter test (average ± standard deviation).

Wire	Ball diameter [μm]	Ball height [μm]	Shear force [g]	Pull force [g]	Pull test failure mode
Au	44.3 ± 0.3	6.8 ± 0.6	16.0 ± 0.5	9.5 ± 0.2	All neck break
Cu	42.4 ± 0.6	12.2 ± 0.6	13.8 ± 0.5	10.9 ± 3.1	8 pad lifts (33.3%)

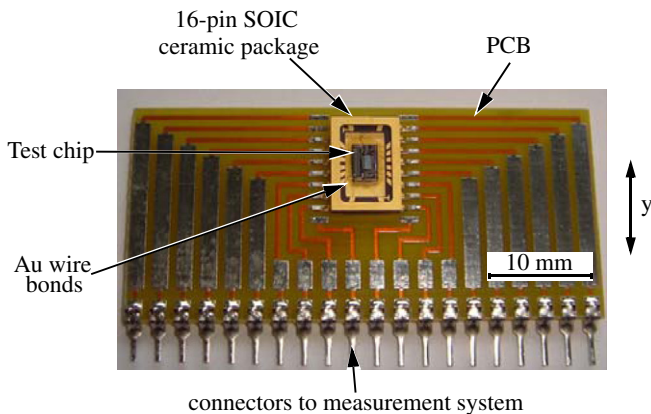


Fig. 1. Microsensor test chip in package, y indicates the ultrasonic direction.

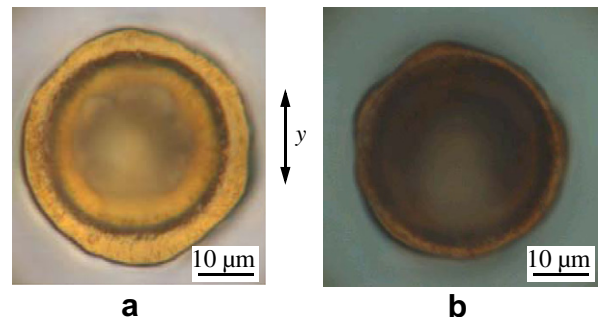


Fig. 2. Typical micrographs of (a) Au and (b) Cu ball bonds made on the microsensor test pad with same set of parameters as shown in Table 1. y indicates the ultrasonic direction.

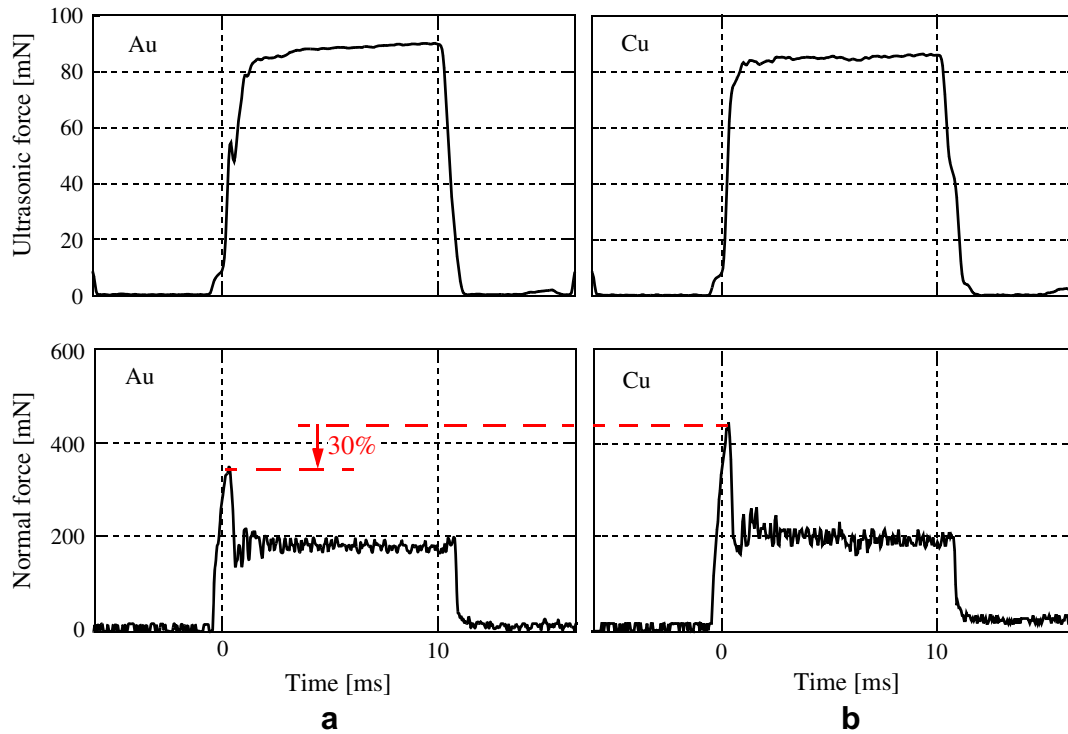


Fig. 3. Ultrasonic and normal force signals for (a) Au and (b) Cu ball bonds made with parameters specified in Table 1.

respectively. The results of ultrasonic force are quite similar for both Au and Cu ball bonding process. In fact, the ultrasonic force measured during Au ball bonding is slightly higher than that in Cu. This indicates that the material properties such as hardness alone cannot be a cause of higher pad stress, and that the differences in the bondability and bonding parameters required for the Cu process might be more influential. To achieve optimal bonding results, the Cu process requires higher force and USG energy, which are the main causes of pad damage.

While the steady state normal force is similar for both processes, the peak value (impact force) measured for the Cu process is $\approx 30\%$ higher than that for the Au process. The bonding machine parameters determining the impact force are contact velocity and contact threshold (touchdown force). After the touchdown of FAB to the bond pad is detected at the contact threshold setting, the machine needs to switch from trajectory control to bond force control. The impact force is the product of an inertial effect between touchdown and bond force. Since Cu has higher yield strength than Au, less FAB deformation upon impact is expected and in shorter time, resulting in a higher reaction force peak (i.e. impact force). It is as if the higher strength and hardness of the Cu causes more of a bounce back effect to the bondhead upon impact than the Au. Instead of an actual bounce back, a higher impact force is recorded. This higher impact force in Cu is not directly related to ultrasonic pad damage or splash. Differences in the material properties of Au and Cu cause strain rate variations during FAB deformation leading to different deformed ball geometries (ball diameter and ball height). Thus, significantly higher settings of contact velocity and/or contact threshold are required during Cu ball bonding to obtain similar bonded ball (BB) geometry (ball diameter and ball height) compared to that in Au ball bonding.

3.1. BB-to-FAB volume

Example SEM micrographs of the typical FABs and BBs made using Au and Cu wires are shown in Figs. 4 and 5, respectively.

The average diameter of the FAB made using Au wire is $39 \pm 1 \mu\text{m}$ and that for Cu wire is $37 \pm 1 \mu\text{m}$. Though the Au FAB is slightly larger than the Cu FAB, the volume of Au BB is much smaller than Cu as indicated by the height of the collar C as shown in Fig. 5a. This is caused by the plastic flow of Au FAB inside the capillary chamfer during the bonding process. Since Au is soft, it is easily squeezed inside the capillary during the FAB deformation process compared to the harder Cu FAB.

The volumes of the FAB and BB are calculated using

$$V_f = \frac{4}{3} \pi (r_f)^3 \quad (1)$$

$$V_b = \pi (r_b)^2 h_b \quad (2)$$

where V_f is FAB volume, r_f is FAB radius, V_b is BB volume, r_b is BB radius, and h_b is the BB height.

Using the measured FAB diameters and BB geometry measurements (Table 2), the volumetric ratio V_b/V_f is 33% and 64% for the Au and Cu ball bonding processes, respectively. This result indicates that while a significant amount of Au FAB deforms inside the capillary chamfer, in the case of Cu, it is outside the capillary as a BB. The difference in V_b/V_f is exaggerated in this test since the parameter settings are larger than optimal for Au and smaller than optimal for Cu. When converting from a Au process to a Cu process, this phenomenon should be kept in mind. Instead of using

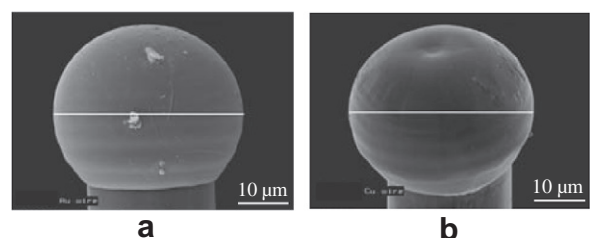


Fig. 4. SEM micrographs of free air balls made with (a) Au and (b) Cu wires.

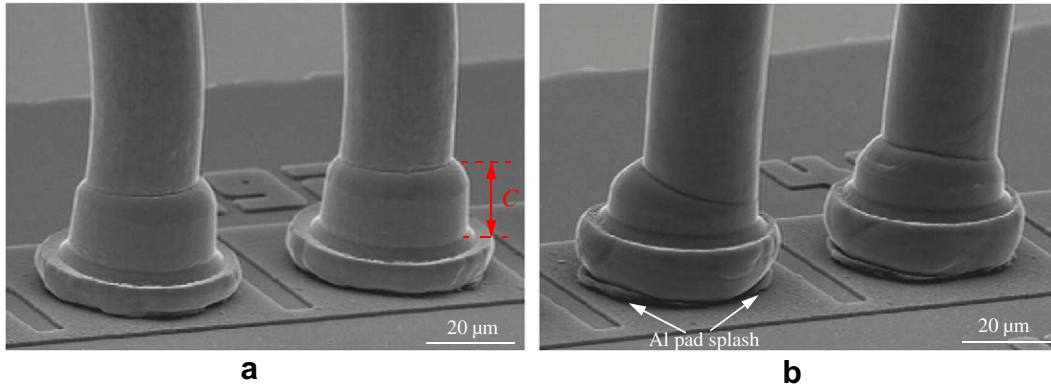


Fig. 5. SEM micrographs of typical bonded balls made using same parameters with (a) Au and (b) Cu wires.

the same FAB diameter for both Au and Cu processes, the Cu FAB can be made slightly smaller than the Au FAB.

3.2. Pad splash

Another observation that can be made from the SEM image shown in Fig. 5b is the amount of Al pad extrusion (pad splash) [15–17] observed in Cu ball bonding. The pad splash is defined as the Al pad material being squeezed outside the BB contact perimeter. Although it is not an indication of failure [25], it generally causes localized pad thinning [17], which reduces the bond reliability and is also an indication of pad damage risk.

The Al pad splash is a phenomenon of metal wear that occurs due to the plastic displacement of surface and near-surface material. The Al pad wear volume W_{wear} be studied using the sliding wear model [26]

$$W = \frac{kLD}{3H} \quad (3)$$

where k is the dimensionless wear coefficient, L is the normal load (in g), D is the sliding distance (in m), and H is the hardness of the softer material (in Pa), in this case the Al bond pad.

The values of hardness of the FAB and BB for Au and Cu wires, and that of the Al bond pad are given in Table 3. The hardness of the FAB is a function of the EFO current and firing time [27]. Due to strain hardening of the FAB during impact deformation, the BB hardness is higher than the FAB hardness. Moreover, the value of hardness is higher at the outside edge of the ball compared to the inner due to higher stress applied by the capillary chamfer at the outer locations during the ball deformation process [17]. While the hardness of the Au BB and Al pad are similar, the hardness of Cu BB is at least 25% higher than that of the Al pad.

For Au and Cu ball bonds made using the same parameters (Table 1), the values of L and D are equal.

Moreover, the value of Al pad hardness H is also same for both Au and Cu processes. Hence, from Eq. (3), the only variable that might contribute to pad splash in this case is the wear coefficient k . The wear coefficient k : represents the probability that a surface asperity is worn away when two materials slide against each other. Typical values of k for fretting wear range from 0.33×10^{-4} for the

Au–Al process [29] to 1×10^{-4} for the Cu–Al process [29]. Thus, even while bonding with same parameters, the value of W for Cu bonding is ≈ 3 times as high as that during the Au bonding. However, given the large uncertainty associated with the values of k in literature [29], quantification of W requires more work to find the values of k specific to Au–Al and Cu–Al bonding processes.

Based on Eq. (3), we can theorize a few different ways to reduce Al splash. These include reducing the normal load (BF), decreasing the sliding distance (depends on synergistic effect of BF and USG), and increasing the hardness of the bond pad. The solution of increasing the hardness of the bond pad has been explored in [30]. It has been shown that Ni/Pd, Ni/Pd/Au, and Ni/Au bond pads are robust for Cu ball bonding. Cu ball bonds made on these pads do not show any splash and possess excellent reliability. In the next section, methods to reduce pad splash in Cu ball bonding on Al pads by modifying and controlling the various process parameters are explored.

4. Design of experiment

To understand the effect of bonding parameters such as impact force (IF), bond force (BF), ultrasound (USG) and FAB size on bonding quality, pad stress and pad splash, a constant diameter design of experiment (DOE) is conducted with Cu wire. Unlike a conventional DOE in which the process responses are not constrained, in this study the process parameters are selected in such a way that BB diameter is constant at $44 \pm 1 \mu\text{m}$. Such a DOE is ideal for analyzing parameter trade-offs while meeting the specifications of a target process. In addition to conventional bonding parameters, the effect of a non-zero USG on impact (pre-bleed USG) is investigated. An example normal force and USG profiles for a bonding process with the amplitude of pre-bleed USG are shown in Fig. 6. Pre-bleed USG helps in reducing the risk of pad damage by producing softer deformed Cu balls after impact due to the usual amount of strain hardening being reduced by the ultrasound during the impact deformation (“acoustic softening”) [31–33].

The parameters settings for the DOE are shown in Table 4. The first three cells are performed with high IF. The 1st cell is high BF and low USG combination, 2nd cell is medium BF and medium USG, 3rd cell is low BF and high USG. Cells 4–6 are low IF cells with varying BF and USG combinations similar to cells 1–3. Cells 7–9 explore the influence of V_b/V_f bonding quality, pad stress and pad splash. The EFO firing time parameter in cell 7 is set to a low value, resulting in a smaller FAB diameter. To get to the target BB diameter, a high USG level is used. In a similar way, cells 8 and 9 explore the effect of medium and large FAB diameter. The last four cells in the DOE explore the settings of pre-bleed USG, which is varied between 0% (no pre-bleed) to 100%.

Table 3
Comparison of Vickers hardness values of FABs, BBs and Bond pad.

Material	FAB hardness	BB hardness
Au	60 Hv [16]	70–80 Hv [16,27]
Cu	80 Hv [16]	100–128 Hv [16]
Al bond pad	70–80 Hv [28]	

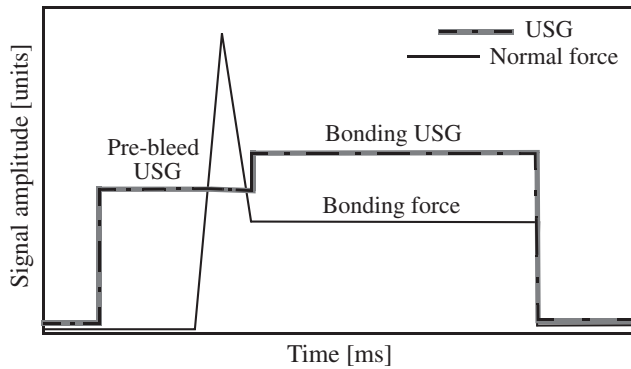


Fig. 6. Illustration of normal force and amplitude of USG showing bonding USG and pre-bleed USG.

Table 4
Bond parameter settings for the DOE.

DOE cell	Contact threshold [machine unit]	Bond force [g]	US [mA]	Pre-bleed USG [%]	EFO firing time [μ s]
1	20	25	75	50	196
2	20	16	95	50	196
3	20	7.5	115	50	196
4	10	25	90	50	196
5	10	16	105	50	196
6	10	7.5	120	50	196
7	16	16	105	50	192
8	16	16	100	50	196
9	16	16	87.5	50	200
10	16	16	105	0	196
11	16	16	100	25	196
12	16	16	95	75	196
13	16	16	90	100	196

The bond time for all cells is fixed at 10 ms. The bonding USG setting is adjusted in each case to achieve the targeted BB diameter. The number of replications for each DOE cell is 24. The measured process responses include ball diameter, ball height, shear/area, pull force, pull test failure mode, and the amount of Al pad splash S_{Al} . The value of $S_{Al} = SD - BDC$, where SD is the maximum splash diameter and BDC is the bonded ball diameter as shown in Fig. 7.

Table 5 summarizes the results of the DOE. The pull test results show a large number of pad lifts. This is a direct indication of pad damage. The USG current plays an important role in determining both the bond strength and pad splash. At low USG levels, i.e. USG < 90 mA (cells 1 and 9), ball lifts are observed. This is due to poor intermetallics formation between Cu and Al at low USG settings. For bonds with high USG settings (>100 mA), pad lifts are predominant. In fact, 8 out of the 13 cells show pad lifts. High USG levels also lead to high values of S_{Al} . This confirms that pad damage is a major issue in Cu ball bonding. The process window between ball lift and pad lift is small.

To obtain the targeted BB diameter using a smaller FAB (Cell 7), a higher value of USG is used. This results in very high S_{Al} (4.7 μ m). Bonded balls made with larger FABs (cell 9) lead to lower values of S_{Al} , however, the number of ball lifts are also high. Bonded balls made with medium FAB diameter (cell 8) seems to give best responses in terms of both S_{Al} and ball lifts.

4.1. Effect of pre-bleed USG

The most influential parameter in the DOE is pre-bleed USG. Fig. 8a and b shows the SEM micrographs of the Al pad after the

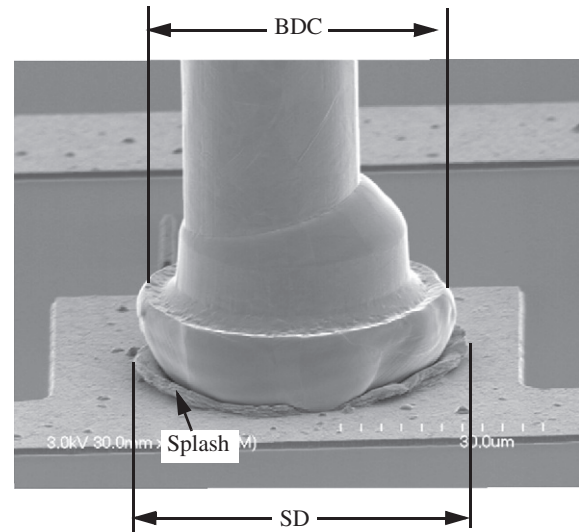


Fig. 7. SEM micrograph of an example Cu ball bond illustrating the maximum splash diameter (SD) and bonded ball diameter measured at capillary imprint (BDC). The pad splash is calculated using $S_{Al} = SD - BDC$.

Table 5
Process responses (average values) for the DOE.

DOE cell	Ball diameter [μ m]	Ball height [μ m]	Shear/area [μ m ²]	Pull force [g]	Pull test failure mode		Al splash [μ m]
					Ball lift [%]	Pad lift [%]	
1	44.3	12.1	4.8	10.2	62.5	0	0
2	44.6	12.1	6.6	12.7	0	4.2	3.0
3	44.7	11.6	7.7	12.4	0	12.5	3.8
4	44.1	12.6	7.3	13.2	0	0	2.4
5	43.6	12.0	8.3	12.8	0	8.3	5.0
6	44.3	12.4	8.0	12.5	0	8.3	2.7
7	43.7	10.3	8.0	13.0	0	0	4.7
8	44.0	11.8	7.3	13.0	0	0	2.9
9	44.5	13.7	6.1	12.7	4.2	0	0.4
10	44.4	12.8	6.8	12.7	0	4.2	3.0
11	44.3	12.9	6.6	12.7	0	4.2	1.8
12	44.3	11.1	7.3	13.1	0	0	2.9
13	45.0	11.3	7.2	13.0	0	0	0.8

Cu BBs are etched away for bonds made with 0% pre-bleed USG and 100% pre-bleed USG, respectively. It is observed that the higher pre-bleed setting reduces Al depletion at the edge of the ball. Pre-bleed also allows the formation of a flatter ball/pad interface instead of a concave-shaped interface as shown in Fig. 9. The concave-shaped interface is undesirable since it is an indication of pad wear near the edge of the bond and poor bonding at the center of the bond. Pre-bleed USG enables the propagation of USG scrubbing from the ball center to the edge. The use of pre-bleed USG also enables a lower bonding USG level to achieve the same ball diameter, which according to Eq. (3) reduces the sliding distance D , thereby reducing Al pad wear.

4.2. Cu Ball bond quality monitoring

Another observation is that a high shear strength is not always a good indication of a high quality bond. In Au wire bonding, high shear per area is often desirable and it is an indication of strong intermetallics formation. In Cu wire bonding, however, pad damage does not usually show up as low shear. Therefore, some of the high shear cells (cells 5 and 6) in this DOE produce some of the most damaged pads. The DOE cells with best responses in

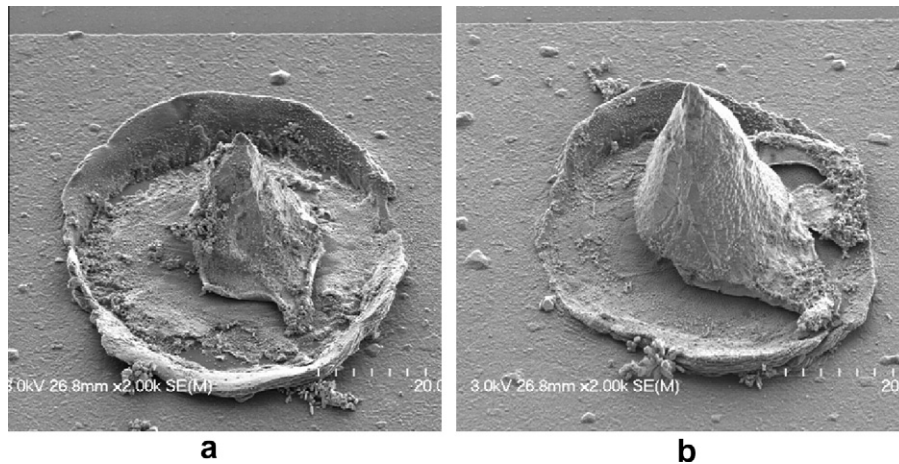


Fig. 8. SEM micrographs of Al bond pad after the Cu ball bonds are etched away: (a) 0% pre-bleed USG and (b) 100% pre-bleed USG.

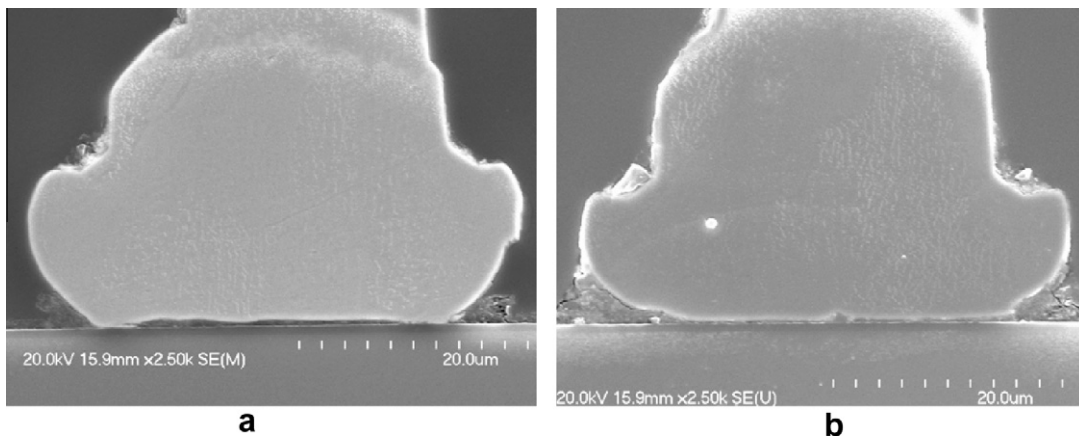


Fig. 9. SEM micrographs of cross-sectioned Cu bonded balls: (a) 0% pre-bleed USG and (b) 100% pre-bleed USG.

terms of both bondability and S_{AI} are those with a shear/area of $\approx 7 \text{ g/mil}^2$. Therefore, in Cu wire bonding, the goal of process optimization should be adequate shear with minimal pad damage, not the highest shear. Pull test for the ball bond should almost always be used to compliment the shear test results.

5. Conclusions

Cu wire bonding provides many cost and performance advantages over Au wire. It also brings along a set of challenges due to its mechanical and chemical properties. To meet these challenges, state-of-art technology along with modeling, in-depth test and analysis will help bring better understanding of Cu wire bonding and unique solutions for Cu bonding process. This paper highlights some differences between Au and Cu bonding process and proposed some solutions and recommendations. When converting a Au process to a Cu process, one should consider reducing Cu FAB size as well as set a higher ball height target due to less material flow inside the capillary. Bonding parameters, such as BF and USG settings need to be kept at low levels to minimize pad stress and pad wear. When optimizing Cu wire bonding, adequate shear with minimal pad damage must be the criterion, instead of the usual highest shear. The pull test at the 1st bond is a good test to reveal pad damage; it should be used to compliment the shear test. The application of pre-bleed USG reduces Al pad wear and im-

proves process window, and it should be considered for Cu wire bonding.

Acknowledgments

This work is supported in part by Natural Sciences and Engineering Research Council of Canada (NSERC), Initiative for Automotive Manufacturing Innovation of Ontario (IAMI) and Ontario Centers of Excellence (OCE). Generous financial support in the form of Government of Canada's NSERC Alexander Graham Bell Canada Graduate Scholarship and University of Waterloo President's Graduate Scholarship is gratefully acknowledged.

The authors would like to thank Virginia Mota for the metrology support and Son Nguyen for the cross-sectioning of the bonds. The helpful input and feedback from Bob Chylak and Horst Clauberg are deeply appreciated.

References

- [1] Greig WJ. Integrated circuit packaging, assembly and interconnections. Springer Science + Business Media; 2007.
- [2] Harman G. Wire bonding in microelectronics materials, processes, reliability, and yield. 2nd ed. New York: McGraw-Hill; 1997.
- [3] Zhou Y, editor. Microjoining and nanojoining. Cambridge (England): Woodhead Publishing Ltd.; 2008.
- [4] Chylak B. Developments in fine pitch copper wire bonding production. In: Proceedings of 11th electronic packaging technology conference; 2009.

- [5] Uno T, Terashima S, Yamada T. Surface-enhanced copper bonding wire for LSI. In: Proceedings of the electronic components and technology conference; 2009. p. 1486–95.
- [6] Moon JT, Hwang JS, Cho JS, Kim SH. New materials for bonding wire. In: Proceedings of semicon Singapore; 2008.
- [7] Nguyen LT, McDonald D, Danker AR, Ng P. Optimization of copper wire bonding on Al–Cu metallization. *IEEE Trans Compon Pack Manufact Technol* 1995;18(2):423–9.
- [8] Kaimori S, Nonaka T, Mizoguchi A. The development of Cu bonding wire with oxidation-resistant metal coating. *IEEE Trans Adv Pack* 2006;29(2):227–31.
- [9] Srikanth N, Murali S, Hong YM, Vath CJ. Critical study of thermosonic copper ball bonding. *Thin Solid Films* 2004;462–463:339–45.
- [10] Deley M, Levine L. The emergence of high volume copper ball bonding. In: Proceedings of semicon west conf; 2004.
- [11] Wong ZW. Wire bonding using copper wire. *Microelectron Int* 2009;26(1):10–6.
- [12] Shah A, Mayer M, Zhou Y, Hong SJ, Moon JT. Low-stress thermosonic copper ball bonding. *IEEE Trans Electron Pack Manufact* 2009;32(3).
- [13] Tan CM, Er E, Hua Y, Chai V. Failure analysis of bond pad metal peeling using FIB and AFM. *IEEE Trans Compon Pack Manufact Technol* 1998;21(4):585–91.
- [14] Tan CM, Linggajaya K, Er E, Chai V. Effect of BOE etching time on wire bonding quality. *IEEE Trans Compon Pack Technol* 1999;22(4):551–7.
- [15] Wulff FW, Breach CD, Stephan D, Saraswati, Dittmet KJ. Characterisation of intermetallic growth in copper and gold ball bonds on aluminum metallisation. In: Proc IEEE electron packag tech conf; 2004.
- [16] Wulff FW, Breach CD, Stephan D, Saraswati, Dittmet KJ, Gamier M. Further characterisation of intermetallic growth in copper and gold ball bonds on aluminum metallisation. In: Proc SEMI tech symp; 2005.
- [17] Hang CJ, Wang CQ, Mayer M, Tian YH, Zhou Y, Wang HH. Growth behavior of Cu/Al intermetallic compounds and cracks in copper ball bonds during isothermal aging. *J Microelectron Reliab* 2008;48:416–24.
- [18] Tan CW, Daud AR. Bond pad cratering study by reliability tests. *J Mater Sci Mater Electron* 2002;13(5):309–14.
- [19] Caers J, Bischoff A, Falk J, Roggen J. Conditions for reliable ball/wedge copper wire bonding. In: Proc IEEE/CHMT Eur int electron man tech symp; 1993. p. 312–5.
- [20] Ho HM, Tan YC, Tan WC, Goh HM. Investigation of factors affecting bonded ball hardness on copper wire bonding. In: Proc IMAPS conf on microelectron packag, Taiwan; 2006.
- [21] Qin I, Shah A, Huynh C, Meyer M, Mayer M, Zhou Y. Effect of process parameters on pad damage during Au and Cu ball bonding processes. In: Proc IEEE electron packag tech conf; 2009.
- [22] Shah A, Lee J, Mayer M, Zhou Y. Online methods to measure breaking force of bonding wire using a CMOS stress sensor and a proximity sensor. *Sensors Actuat A Phys* 2008;148:462–71.
- [23] Shah A, Mayer M, Zhou Y, Hong SJ. In-situ ultrasonic force signals during low temperature thermosonic copper wire bonding using piezo-resistive microsensors. *Microelectron Eng* 2008;85(9):1851–7.
- [24] Schwizer J, Mayer M, Brand O. Force sensors for microelectronic packaging applications. Series: microtechnology and MEMS. New York: Springer Science; 2005.
- [25] England L, Jiang T. Reliability of Cu wire bonding to Al metallization. *Proc Electron Compon Technol Conf* 2007:1604–13.
- [26] Archard JK. Contact and rubbing of flat surfaces. *J Appl Phys* 1953;24:981–8.
- [27] Zhong ZW et al. Study of factors affecting the hardness of ball bonds in copper wire bonding. *Microelectron Eng* 2007;84(2):368–74.
- [28] Quality control of integrated circuit (IC), bonding pads with the nano hardness tester (NHT) from CSM instruments; 2006 <<http://www.azonano.com/>>.
- [29] Rabinowicz E. Wear coefficients – metals. In: Peterson MB, Winer WO, editors. *Wear control handbook*. New York: American Society of Mechanical Engineers; 1980. p. 475–506.
- [30] Chylak B, Ling J, Clauberg H, Thieme T. Next generation nickel-based bond pads enable copper wire bonding. *ECS Trans* 2009;18(1):777–85.
- [31] Lum I, Huang H, Chang B, Mayer M, Du D, Zhou Y. Effects of superimposed ultrasound on deformation of gold. *J Appl Phys* 2009;105:024905.
- [32] Lum I, Hang CJ, Mayer M, Zhou Y. In-situ studies of the effect of ultrasound during deformation on residual hardness of a metal. *J Electron Mater* 2009;38(5):647–54.
- [33] Huang H, Pequegnat A, Chang BH, Mayer M, Du D, Zhou Y. Influence of superimposed ultrasound on deformability of Cu. *J Appl Phys* 2009;106:113514.